
Article:
Slattery, John Martin orcid.org/0000-0001-6491-8302, Leeb, Nina Maria, Drover, Marcus et al. (2 more authors) (2018) Phosphoramidate-assisted alkyne activation: Probing the mechanism of proton shuttling in a N,O-chelated Cp*Ir(III) complex. Organometallics. ISSN 0276-7333

https://doi.org/10.1021/acs.organomet.8b00656

Phosphoramidate-assisted alkyne activation: Probing the mechanism of proton shuttling in a *N,O*-chelated Cp*Ir(III) complex

Nina M. Leeb,[1] Marcus W. Drover,[2,3] Jennifer A. Love,[2] Laurel L. Schafer[2] and John M. Slattery[1,*]

[1] Department of Chemistry, University of York, Heslington, York, YO10 5DD, UK. Email: john.slattery@york.ac.uk. Tel: +44 (0)1904 322610
[2] Department of Chemistry, The University of British Columbia, 2036 Main Mall, Vancouver, British Columbia, Canada, V6T 1Z1
[3] Division of Chemistry and Chemical Engineering, California Institute of Technology, Pasadena, California, 91125, USA

TOC figure

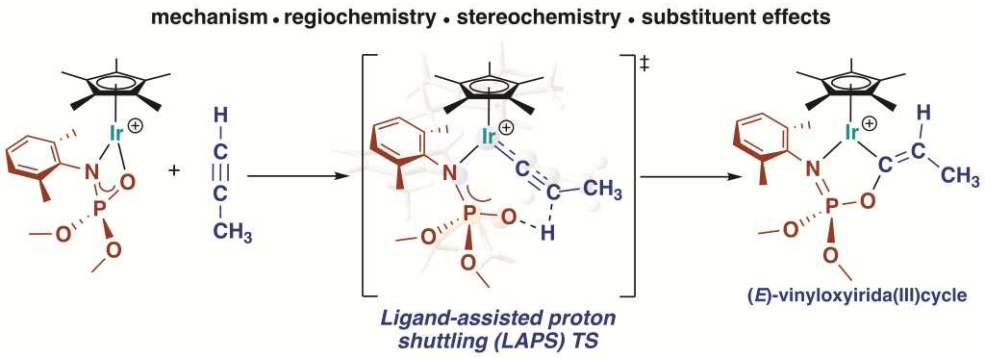

Abstract

Ligand lability offers a unique opportunity for access to metal-ligand cooperativity (MLC), helping to direct new organometallic and catalytic reactions. In recent years, ligand-assisted C-H bond activation, and more generally, proton migration, have been of particular interest. This contribution describes a detailed computational study into the mechanism, regio-, and stereoselectivity observed in a recently reported transformation where MLC in a 16-electron iridium(III) phosphoramidate complex plays a critical role in directing the activation of terminal alkynes toward the generation of novel five-membered (*E*)-vinyloxyirida(III)cycles. Five possible pathways for the formation of such products were investigated. Based on our findings, it is proposed that the reaction proceeds *via* a ligand-assisted proton shuttle (LAPS) mechanism, where the phosphoramidate phosphoryl (P=O) group assists in both alkyne C-H bond activation and C-H bond formation to form a vinylidene intermediate. Next, C-O bond

formation occurs *via* nucleophilic attack at the α-carbon of the vinylidene giving the observed product. Although C-N (and not C-O) bond formation is thermodynamically favored in this model system, this trend is not observed experimentally and the computational study suggests that the observed regioisomer is simply the kinetic reaction product. In terms of stereoselectivity, formation of the (*E*)-irida(III)cycle is explained by its thermodynamic stability, when compared to the (*Z*)-isomer, and the relatively low barrier to interconversion between them.

Introduction

Metal-based reactivity underpins organometallic chemistry and catalysis, but in some cases ligand systems play more than a supporting role, directly facilitating reactions alongside the metal. This metal-ligand cooperativity (MLC) can take a variety of forms.[1] For example, it may involve redox-active ligands such as nitrosyls or dithiolenes,[2-5] or ligands that promote bond activation or formation, as is observed for some transfer hydrogenation catalysts or in pincer ligand complexes that undergo ligand aromatization/dearomatization reactions.[6-9] A sub-class of MLC that has been of significant interest in recent years involves ligands that are able to facilitate C-H bond activation, and in some cases subsequent E-H bond formation, by acting as intramolecular bases that work alongside a metal to deprotonate a C-H bond, forming a M-C bond.[10-12] Such ligands are often hemilabile, stabilizing the metal by chelation when required, but switching denticity to allow ready access to the metal for incoming substrates and to facilitate proton migrations. Examples of this behavior are seen in the concerted metallation deprotonation (CMD) and ambiphilic metal-ligand activation (AMLA) mechanisms,[13,14] which commonly involve late transition metal carboxylate complexes (Figure 1, A). These are important in a range of stoichiometric and catalytic C-H bond activation and functionalization reactions.[15,16] An alternative, but related, mechanism for C-H bond activation has been termed ligand-to-ligand hydrogen transfer (LLHT). For example, LLHT is proposed to occur as part of the catalytic cycle in alkyne hydrofluoroarylation reactions catalyzed by a nickel-phosphine complex (Figure 1, B).[17] In this unusual case, an alkyne ligand acts as the proton acceptor during the C-H bond activation of a fluoroarene, rather than a heteroatom-bearing ligand such as acetate.

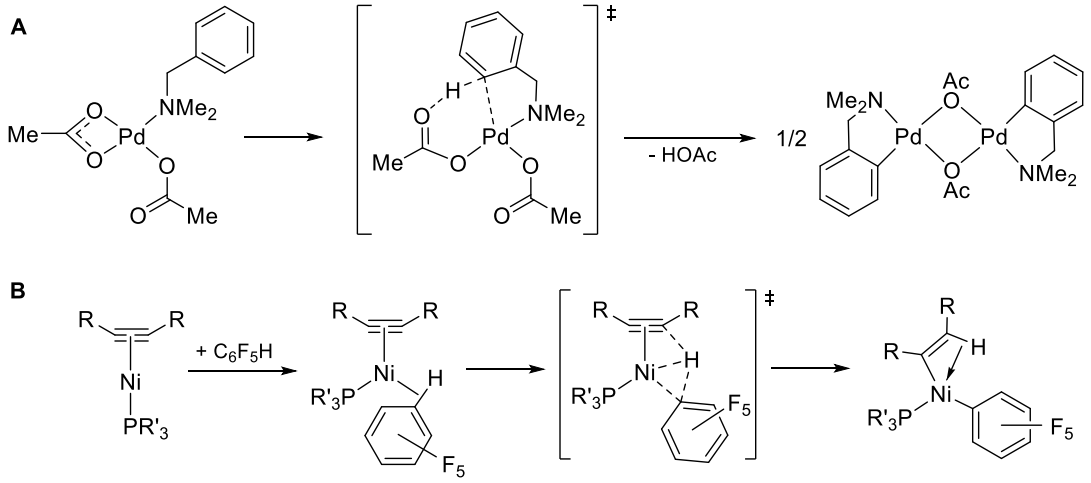

Figure 1: (**A**) An example of a CMD/AMLA mechanism, involving an acetate-assisted C-H bond activation, in the reaction between *N*,*N*-dimethylbenzylamine and $Pd(OAc)_2$.[18] (**B**) The LLHT mechanism that is part of the proposed catalytic cycle for the hydrofluoroarylation of alkynes by Ni(0).[17]

In many CMD/AMLA reactions the protonated ligand is subsequently lost from the metal. However, it is also possible for this unit to remain bound and to act as an intramolecular acid, protonating a basic site on the substrate. Examples of this type of behavior are seen in the ligand-assisted proton shuttle (LAPS) mechanism (Figure 2). Such proton shuttling can facilitate a range of reactions. LAPS has been proposed to underpin some alkyne-vinylidene tautomerisations,[19] the hydration of terminal alkynes catalyzed by a ruthenium complex bearing a self-assembled ligand system,[20] and to explain the different reactivity towards terminal alkynes of $[Ru(X)H(CO)(P^iPr_3)_2]$ (X = Cl or OAc).[21] The latter is a particularly interesting recent development where acetate groups are proposed to transfer a proton between two mutually *trans* ligands at ruthenium.

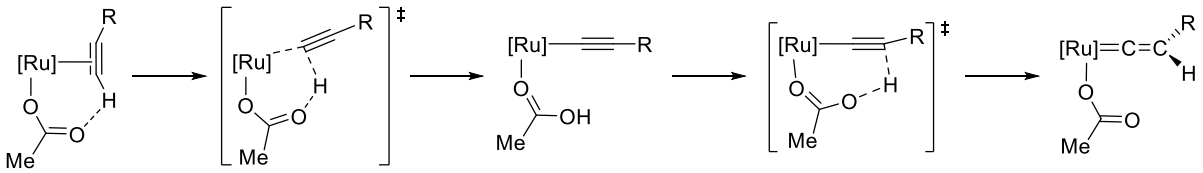

Figure 2: An example of the LAPS mechanism in the reaction of $[Ru(OAc)_2(PPh_3)_2]$ with terminal alkynes. [Ru] = [*trans*-$Ru(OAc)(PPh_3)_2$].

Recently, an unsaturated Ir(III) phosphoramidate complex was presented as a system capable of MLC for the development of a new approach to the regio- and stereoselective *O*-phosphoramidation of 1-alkynes.[22] In these reactions, the Ir(III) complex [Cp*Ir(κ^2-*N*,*O*-Xyl(N)P(O)(OEt)$_2$)][BAr$^F_4$] (Ar^F = 3,5-(CF$_3$)$_2$C$_6$H$_3$), Xyl = 2,6-Me$_2$C$_6$H$_3$, [**1**][BAr$^F_4$]) reacts quickly and selectively with terminal alkynes to give (*E*)-vinyloxyirida(III)cycles [**5**][BAr$^F_4$] (Figure 3). The resulting metal complexes not only provide mechanistic insight to the community on related amidation reactions,[23,24] invoking similar intermediates, but also, the organic products from these reactions, vinyloxy organophosphates are acetylcholinesterase inhibitors used as commercial agrochemicals.[25] It was initially proposed that this reaction proceeds *via* a LAPS mechanism, where the phosphoramidate ligand is hemilabile and acts as a proton shuttle to facilitate alkyne C-H bond activation and subsequent tautomerisation. Previous work has shown that similar *N*,*O*-chelated phosphoramidate complexes display hemilabile behavior – a factor that has been harnessed for the activation of small molecules.[26-30] Although, a detailed mechanistic study of the reaction shown in Figure 3 was not performed, it was possible to confirm that the reaction likely proceeds *via* initial π-coordination of the alkyne to [**1**][BAr$^F_4$], as the reaction is inhibited in the presence of a coordinating solvent (MeCN). However, a number of mechanistic proposals remain to be tested and are the subject of the present work.

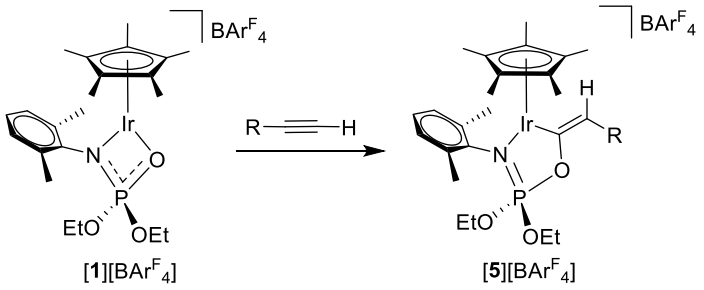

Figure 3: The regio- and stereoselective *O*-phosphoramidation of 1-alkynes at Ir(III).

This work aims to answer, through a comprehensive computational study, a number of mechanistic questions relating to the phosphoramidate-assisted alkyne C-H bond activation shown in Figure 3. It is hoped that this study will aid the development of catalytic protocols based on this novel reactivity and

further the community's understanding of MLC (as it relates to C-H bond activation) in general. Specific questions include:

- Does alkyne activation proceed *via* a ligand-assisted mechanism or a classical mechanism such as C-H bond oxidative addition *via* an Ir(V) hydride complex?
- What is the origin of the regioselective C-O bond formation in this system?
- What is the origin of the (*E*)-stereoselectivity for vinyloxy iridium(III) complex formation?
- How do the 1-alkyne substituent effects influence the energetics for the reaction?

Computational details

Computational studies were performed at the (RI)-PBE0-D3/def2-TZVPP//(RI)-BP86/def-SV(P) level including COSMO solvation (in CH_2Cl_2, ε= 8.93 at 298 K) and DFT-D3BJ corrections.[31-39] Vibrational frequency calculations were used to determine the nature of the stationary points and Dynamic Reaction Coordinate (DRC) calculations were performed to connect transition states to their corresponding minima.[40-42] This is indicated by dashed lines on the potential energy surface (*vide infra*). Where no lines are present, the connection between the transition states and minima have not been verified. The (RI-)PBE0/def2-TZVPP SCF energies were corrected for their zero point energies (ZPE), thermal energies and entropies (obtained from the (RI-)BP86/SV(P)-level frequency calculations). Relative Gibbs energies are discussed in the text below and relative enthalpies are given in brackets on all potential energy surfaces (COSMO CH_2Cl_2 solvation and DFT-D3BJ corrections are included in all reported energies). All calculations were performed using the TURBOMOLE V6.40 package.[43,44] Full computational details can be found in the supporting information.

A slightly simplified model, compared to the system studied by Drover *et al.*,[22] was used for most of the study. The R group of the alkyne was simplified to a methyl group for the mechanistic work, while Ph, *p*-^{t}BuPh, ^{t}Bu and Cy were used in some cases to assess substituent effects (*vide infra*). The alkyl chains of the phosphoramidate were shortened from ethyl to methyl to reduce conformational flexibility without significantly affecting the electronic properties of the ligand. Calculated bond lengths were compared to those obtained from crystallographic data. These differ at most by 0.03 Å, giving

confidence that the computational methodology used reproduces the structural characteristics of the system well.

Results and discussion

The first step in the formation of **5** is coordination of an alkyne to complex **1** to form the 18-electron η^2-C,C adduct **2** (Figure 4). Formation of the κ^1-*N* coordinated, 16-electron isomer of **2** through loss of phosphoramidate *O*-coordination, was found to be slightly favorable, by 10 kJ mol^{-1}, while a stationary point corresponding to loss of phosphoramidate *N*-coordination was not observed. The preference for 16-electron isomers of **2** may be related to the relief of ring strain in the κ^1-coordinated complexes compared to the κ^2-coordinated isomers, reduction of the N(lp) to d-orbital antibonding interactions that are observed in the HOMOs of the κ^2-coordinated complexes or the stabilization afforded by the strong, free P=O bond. From **2**, five potential pathways to give the (*E*)-vinyloxyirida(III)cycle **5** were considered. The first three involve ligand-assisted proton shuttle (LAPS)[19-21] steps (Figure 4, upper panel): 1) the *O*-protonation pathway proceeds *via* deprotonation of the terminal alkyne C-H bond by the phosphoramidate P=O group to give acetylide complex **3a**; 2) the *N*-protonation pathway involves activation of the alkyne C-H bond by the phosphoramidate P-NR group, and finally, 3) the Cp*-protonation pathway involves proton transfer from the alkyne to the Cp* ligand; these result in the formation of acetylide complexes **3b** and **3c,** respectively. The fourth pathway studied involves a direct 1,2-hydride shift to give the vinylidene complex **4** (Figure 4, lower panel), while the final pathway considered is direct C(*sp*)-H bond oxidative addition of the alkyne by Ir(III) to form an Ir(V) hydride intermediate **6** (Figure 4, lower panel).

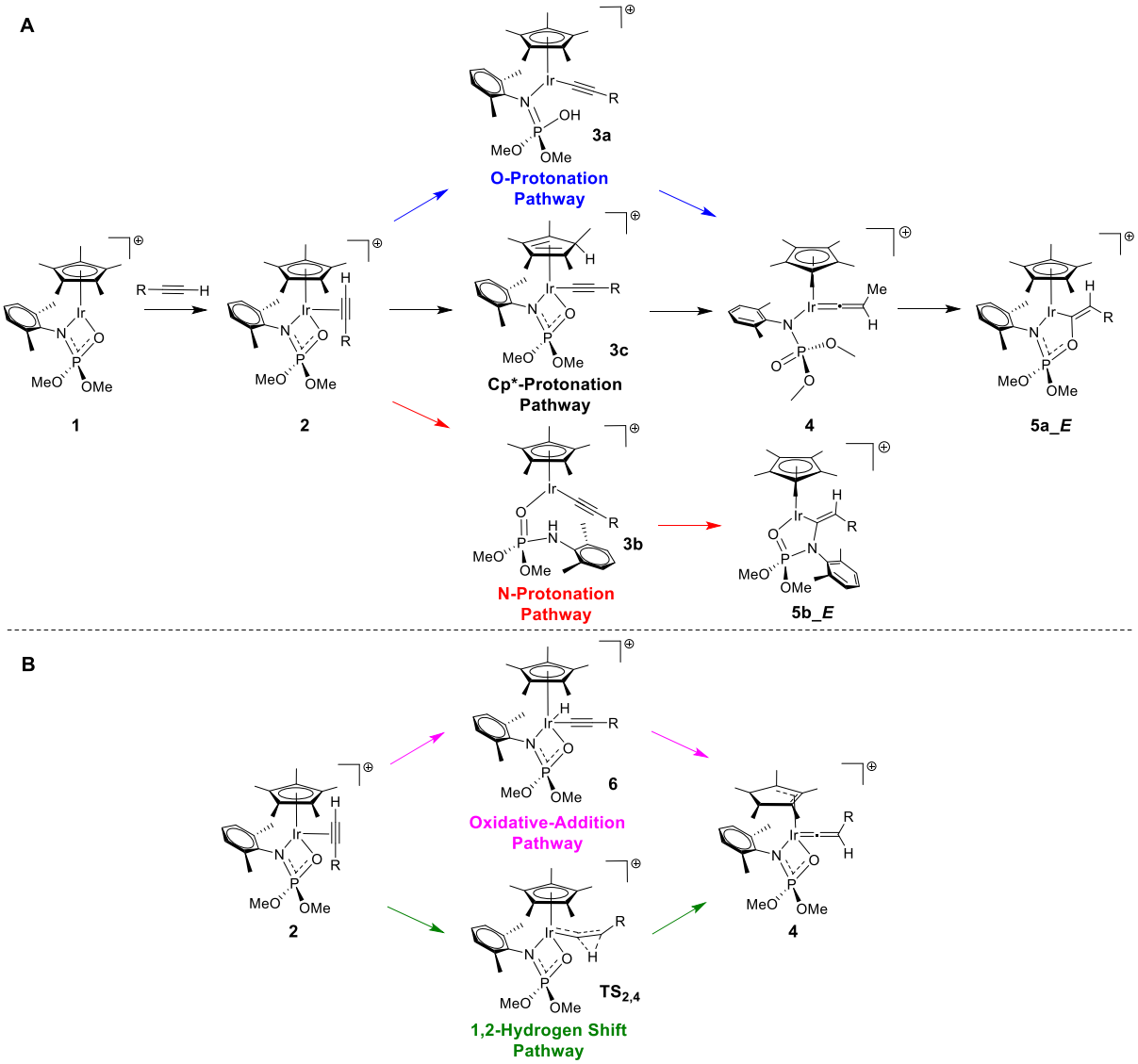

Figure 4: Overview of the different mechanistic pathways considered for alkyne C-H bond activation and formation of **5**. **Upper panel (A):** ligand-directed pathways involving proton migration *via* a non-innocent ligand. **Lower panel (B):** Non-ligand directed pathways involving oxidative addition or direct 1,2-hydrogen migration.

Each of the four pathways that proceed *via* formation of a metal acetylide intermediate can subsequently undergo hydrogen migration, which may (or may not) be ligand-assisted, to form **4** (or in the case of the *N*-protonation pathway to form **5** directly). Such complexes are well known to react with

nucleophilic reagents at the vinylidene α-carbon and it was previously postulated that intramolecular attack of by the phosphoramidate P=O group lead to formation of the observed product **5a_*E***.[22]

Mechanism of alkyne activation

Analysis of the computational data found that two of the five pathways considered; those involving protonation of the Cp* ligand to form **3c** and oxidative addition of the alkyne to form **6** had relatively high barriers ($\Delta G^{\ddagger}$ = 254 and 91 kJ mol^{-1}, respectively) compared to the other pathways (see ESI for full details) and as such, these are not discussed further. The potential energy surface (PES) for the remaining three pathways is shown in Figure 5.

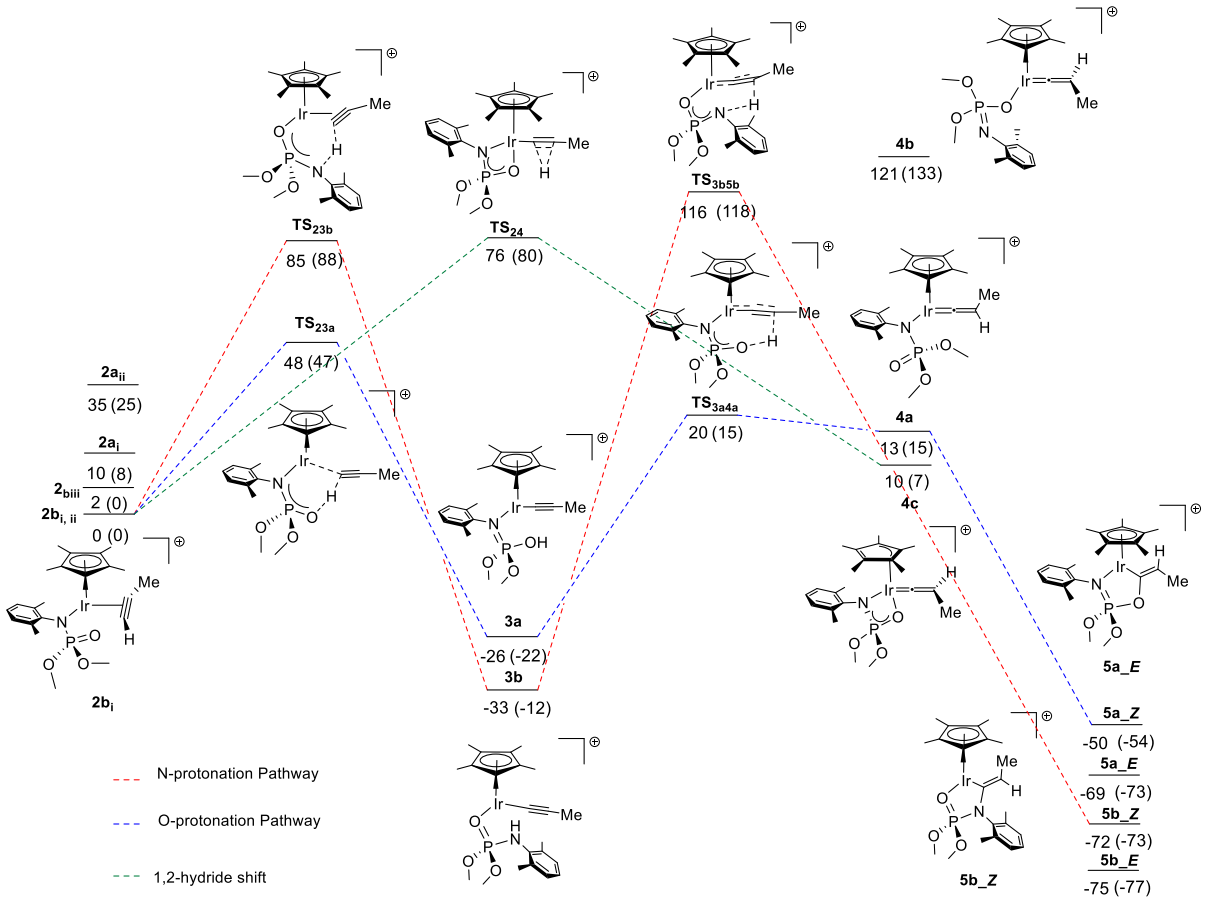

Figure 5: Potential energy surface for three of the five pathways considered for the formation of **5**: *O*-protonation (blue), *N*-protonation (red), and direct 1,2-hydride shift (green). Gibbs energies, relative to **2b$_i$**, are shown in kJ mol^{-1} at the (RI)-PBE0-D3/def2-TZVPP//(RI)-BP86/SV(P) level in CH_2Cl_2 (COSMO solvation). Relative enthalpies, at the same level, are also shown in brackets.

The *O*-protonation pathway initially proceeds *via* **TS_{23a}**, shown in Figure 6, which involves deprotonation of the alkyne C-H bond by the P=O group. The transition state displays a quasi-linear alkynyl < C-C-C angle, but the < Ir-C-C angle is smaller (146°), with the structure being reminiscent of an alkyne C-H σ-complex.[45] The Ir-C distance of 2.10, C-H distance of 1.20, and O···H distance of 1.61 Å suggest a relatively early transition state. Significant shortening of the Ir-N bond from 2.23 to 2.01 Å is observed, which is coupled to an increase in the P-N distance from 1.62 to 1.70 Å. These metrics can be compared to related systems that undergo LAPS or ligand-assisted C-H bond activation (*e.g.* CMD/AMLA) processes. In the reaction of $[Ru(\kappa^2\text{-}OAc)_2(PPh_3)_2]$ with terminal alkynes to give Ru-vinylidene complexes, DFT studies showed later, less "alkyne-like" transition states for acetate-assisted C-H bond activation, with Ru-C, C-H, and O-H distances of 2.07, 1.32, and 1.51 Å, respectively for the *cis*-phosphine pathway and 2.00, 1.29, and 1.44 Å, respectively for the *trans*-phosphine pathway.[19] Similar bond distances were encountered for the first LAPS transition state of the $[Ru(\eta^5\text{-}C_5H_5)$(6-DPPAP)(3-DPICon)$]^+$ (6-DPPAP = 6-(diphenylphosphino)-*N*-pivaloyl-2-aminopyridine, 3-DPICon = 3-diphenylphosphinoisoquinolone) alkyne hydration catalyst system studied by Lynam and Slattery: Ru-C: 2.07, C-H: 1.31 and N-H: 1.41 Å.[20] In a related system involving the reaction of *trans*-$[Ru(P^iPr_3)_2(CO)(\kappa^2\text{-}OAc)(\kappa^1\text{-}E\text{-}CHCHPh)]$ with terminal alkynes,[21] acetate-assisted C-H bond activation occurs *via* a transition state where the hydrogen atom lies equidistant between the carbon and oxygen atoms of the alkyne and acetate, with Ru-C, C-H, and O-H distances of 2.29, 1.29, and 1.31 Å, respectively. The C-H bond activation of benzene involving $Pd(\kappa^2\text{-}O_2CH)_2$ has been proposed to proceed *via* a CMD pathway and a similar metal-carbon distance was reported (2.11 Å) however, the O-H distance was significantly shorter (1.28 Å) than most of the LAPS mechanisms described above.[46] For the ambiphilic metal-ligand assisted (AMLA) cyclometalation of *N,N*-dimethylbenzylamine using $[Cp^*_2IrCl_2]_2$, a similar metal-carbon distance is observed (2.15 Å), but again the O-H distance is significantly shorter (1.30 Å).[10]

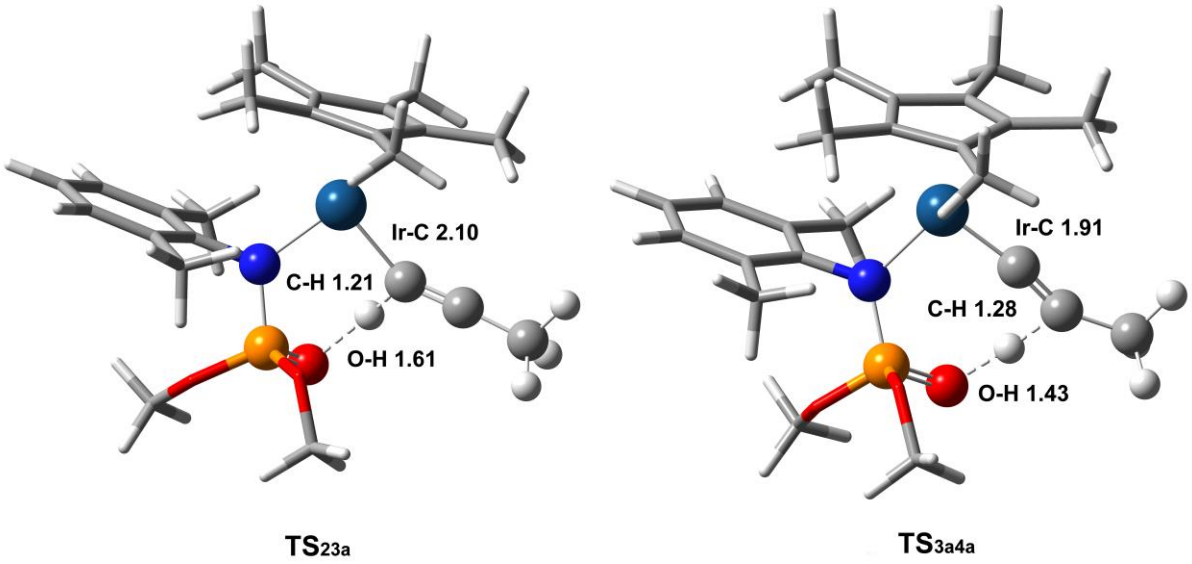

Figure 6: Transition-state structures for the *O*-protonation pathway. Selected distances are shown in Å. Dark blue = Ir, blue = N, orange = P, red = O, grey = C and white = H.

The resulting acetylide complex **3a** lies 26 kJ mol^{-1} lower in energy than the alkyne complex from which it is formed and is stabilized by an OH···π interaction between the protonated phosphoramidate ligand and acetylide. Next, complex **3a** undergoes the second step of LAPS, where the acetylide β-carbon is protonated by the P-OH group, *via* $\mathbf{TS_{3a4a}}$ to give vinylidene **4a**. Indicative of vinylidene formation, analysis of $\mathbf{TS_{3a4a}}$ shows that there is a slight lengthening of the C-C bond from 1.28 to 1.32 Å and a shortening of the Ir-C distance from 1.91 to 1.86 Å. Further, the hydrogen atom involved in the LAPS step lies closer to O than C with O···H and C···H distances of 1.28 and 1.43 Å, respectively. Related systems that undergo LAPS processes show similar metric parameters for equivalent transition states, although the position of the proton between C and heteroatom varies. For example, reaction of $[Ru(\kappa^2\text{-}OAc)_2(PPh_3)_2]$ with terminal alkynes, (*trans*-isomer pathway) shows that the hydrogen atom lies closest to the acetate oxygen (O-H: 1.25 Å *vs.* C-H: 1.44 Å) while in the *cis*-isomer transition state, the hydrogen atom lies closest to the β-carbon (O-H: 1.47 Å *vs.* C-H: 1.30 Å).[19] In a recently reported reaction where acetate ligands assist in proton transfer between two different ligands (from an alkyne to an alkenyl ligand) the transition state for the second LAPS step also involves a relatively short O-H and longer C-H distance (1.22 and 1.41 Å, respectively).[21] In a system where the

proton shuttling site is nitrogen-based, during the second LAPS transition state, the hydrogen atom sits roughly equidistant between nitrogen and the β-carbon (N-H: 1.34 Å *vs.* C-H: 1.39 Å).[20]

A number of isomers for vinylidene **4** were located. **TS_{3a4a}** leads directly to **4a**, which displays κ^1-*N* coordination. This isomer can readily shift to κ^2-*N,O* phosphoramidate coordination through the essentially isoenergetic isomer **4c**, which results in a change in hapticity of the Cp* ligand from η^5 to η^3, maintaining the 16-electron configuration that is favoured for this system. The origin of this hapticity change in **4c** is not clear and κ^2-*N,O* phosphoramidate coordinated isomers of **4** with η^5–Cp* coordination could not be located. A third, higher-energy isomer (**4b**) was also found which displays κ^1-*O* coordination. Rotation around the [Ir]=C bond of the vinylidene is also possible, leading to additional conformational isomers. This is known to be a low energy process in related species,[47,48]and the rotational barrier in the present system has been calculated by us to be around 10 kJ mol^{-1} (see ESI for details). Nucleophilic attack of the P=O group of the κ^1-*N* coordinated phosphoramidate at the α-carbon of the vinylidene in one of these conformational isomers (**4ai**) leads to the observed product **5a_*E*** on the *O*-protonation pathway. A PES scan along the C-O distance in **4ai** showed no barrier for this C-O bond formation process (see ESI for details).

The *N*-protonation pathway is similar to the *O*-protonation pathway and invokes a LAPS mechanism where the P-NR group acts as a proton shuttle to deprotonate the alkyne C-H bond *via* **TS_{23b}** to give the intermediate acetylide **3b**, followed by protonation of the acetylide β-carbon by the phosphoramide P-N(H)R group in **TS_{3b5b}**; Figure 7 depicts the two transition states associated with this pathway. By contrast to the *O*-protonation pathway, a significant degree of κ^2-*N,O* coordination is maintained in **TS_{23b}** (Ir-N distance of 2.37 Å in the TS, compared to 2.23 Å in **2**), which suggests a penalty to breaking the Ir-N bond. Indeed, the barrier to acetylide formation is 37 kJ mol^{-1} higher for the *N*-protonation pathway. Complex **3b** is slightly more stable on the *N*-protonation pathway and the ensuing transition state (**TS_{3b5b}**) has a much higher energy when compared to **TS_{3a4a}**. This is consistent with the N-H protonated phosphoramidate being a weaker acid when compared to the P-O-H unit, and manifests itself in a near three-fold higher barrier for the second LAPS step of 149 kJ mol^{-1} (compared to 48 kJ mol^{-1} for the *O*-protonation pathway). One final, and crucially important, difference on the *N*-

protonation pathway is that $\mathbf{TS_{3b5b}}$ leads directly to **5b_*Z***, which was confirmed by DRC analysis, rather than to a vinylidene isomer. While a high-energy isomer of **4** (**4b**) with κ^1-*O* coordination could be located, this molecule does not lie along the *N*-protonation pathway. This is presumably a consequence of the higher basicity of the P-NR group compared to the P=O group, which leads to barrierless attack at the vinylidene α-carbon by the phosphoramidate P-NR group immediately following proton transfer.

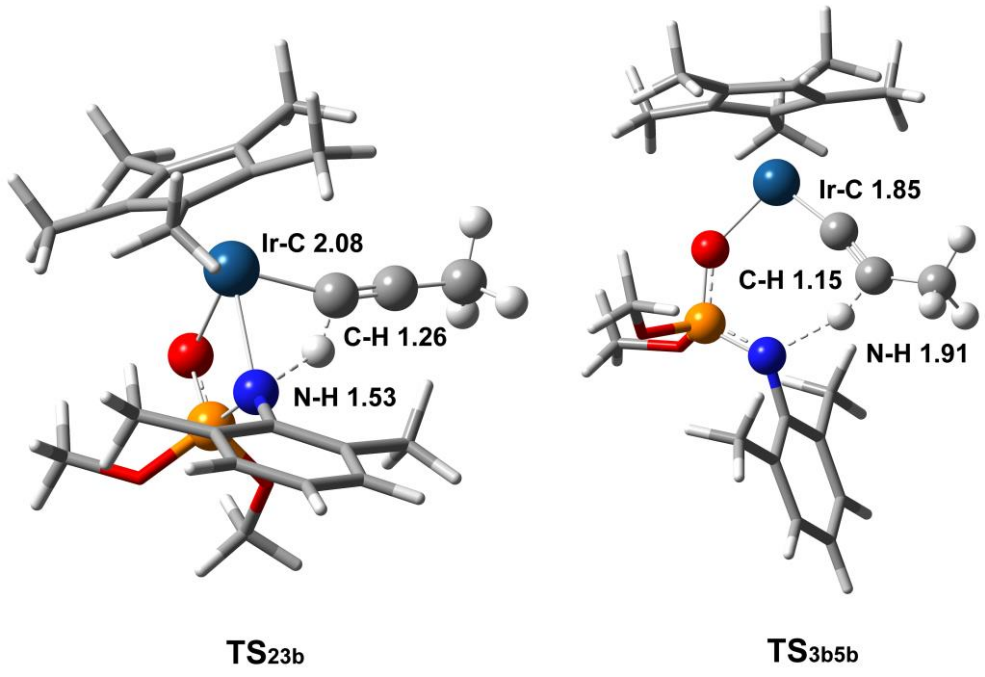

Figure 7: Transition states involved in the *N*-protonation pathway. Selected distances are shown in Å. Dark blue = Ir, blue = N, orange = P, red = O, grey = C and white = H.

The 1,2-hydrogen migration pathway proceeds *via* a single transition state ($\mathbf{TS_{24}}$) that is 76 kJ mol^{-1} higher than $\mathbf{2b_i}$, to give the vinylidene **4c** (Figure 8). The hemilabile phosphoramidate ligand maintains κ^2-*N,O* coordination on this pathway until **4c**, where it may subsequently adopt a κ^1-*N* coordination mode (to form isomer **4a**) to allow for attack of the P=O group at the vinylidene α-carbon, forming **5a**. Similar flexibility to form the κ^1-*O* coordination mode appears to be unfavourable in this

system (**4b** lies 111 kJ mol^{-1} higher in energy than **4c**), preventing the formation of **5b** directly from any of the isomers of **4**.

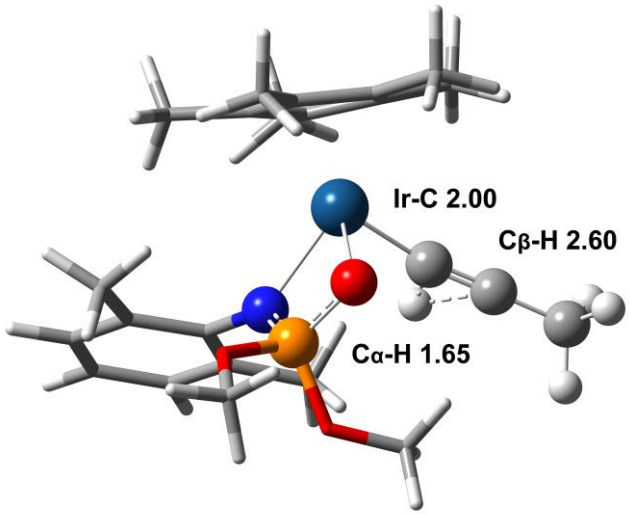

TS$_{24}$

Figure 8: Transition state for the 1,2-hydrogen migration pathway. Selected distances are shown in Å. Dark blue = Ir, blue = N, orange = P, red = O, grey = C and white = H.

In general, Figure 5 shows that the *N*-protonation pathway is associated with a large barrier ($\Delta G^{\ddagger}$ = 149 kJ mol^{-1}) that is not competitive with the other pathways, and indeed is inconsistent with the fast reaction observed experimentally (**5a_*E*** is formed in < 5 min after mixing **1** and phenyl acetylene).[22] In this system, loss of Ir-N coordination to deprotonate the alkyne is significantly less favorable than loss of Ir-O coordination. In addition, the *N*-protonated phosphoramidate appears to be too weakly acidic to protonate the acetylide β-carbon and thus, the *N*-protonation pathway is unlikely to be followed. The 1,2-hydrogen shift pathway has only a modest barrier to vinylidene formation and subsequently **5a_*E*** ($\Delta G^{\ddagger}$ = 76 kJ mol^{-1}). Conversely, the *O*-protonation pathway is significantly lower in energy ($\Delta G^{\ddagger}$ = 48 kJ mol^{-1}, relating to the energy difference between **2b$_i$** and **TS$_{23a}$**). As such, it is reasonable to conclude that **5a_*E*** is formed *via* a LAPS mechanism where the P=O group of the hemilabile phosphoramidate ligand plays a key role as a proton shuttling unit.

Origins of regio- and stereoselectivity

Although a number of isomers of **5** are possible (Figure 9), it was found that **5a_*E*** was the exclusive product from the reaction between **1** and phenylacetylene (neither **5b** nor the (*Z*)-vinyloxyirida(III)cycle were observed) - observations that are independent of the nature of 1-alkyne R group (R = *p*-^{t}BuPh, Cy, ^{n}Bu, and ^{t}Bu). The computational data presented here suggest that **5b_*E*** is the thermodynamic product, although the difference in energy compared to **5a_*E*** and **5b_*Z*** is small. This suggests that **5a_*E*** is the kinetic product of this reaction, with the observed regiochemistry being linked to the mechanism of alkyne tautomerisation and subsequent intramolecular reactivity with the phosphoramidate ligand. Indeed, all of these observations are consistent with the analysis of the PES above. The κ^1-*N* coordinated phosphoramidate isomer of the vinylidene **4a** is formed *via* a LAPS mechanism along the *O*-protonation pathway. This can lead directly to **5a** by attack of the phosphoramidate at the vinylidene α-carbon. However, the *N*-protonation pathway leads directly from **3b** to **5b_Z**, without formation of a vinylidene intermediate. This is indicated by the DRC analysis for **TS$_{3b5b}$**, which shows that the phosphoramidate nitrogen atom undergoes C-N bond formation directly after protonating the acetylide β-carbon. In addition, geometry optimization from the final point of the DRC results in the final product **5b_Z** and not simply an isomer of **4**.

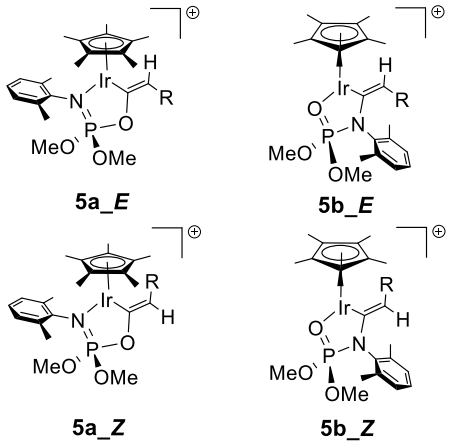

Figure 9: Potential isomers of complex **5**.

It is clear from Figure 5 that the *N*-protonation pathway is significantly disfavored compared to the *O*-protonation pathway. Another route to formation of **5b** would be from a κ^2-*N,O* coordinated phosphoramidate isomer of the vinylidene **4c**, which could shift to κ^1-*O* coordination allowing for attack of the P-NR group at the vinylidene to generate a new C-N bond. However, this would require the formation of the high-energy vinylidene isomer **4b** (108 kJ mol^{-1} higher in energy than **4a**) introducing a significant reaction barrier. PES scans varying the C-O and C-N distances from **4c** were carried out in order to assess the possibility of alternative pathways for C-O or C-N bond formation directly from **4c** (see ESI). In both cases κ^2-*N,O* coordination is maintained until the highest energy point along the scan. In the C-O bond formation scan, η^3-coordination of the Cp* is also maintained up to this point, although in the C-N bond formation scan, the Cp* gradually shifts towards η^5-coordination. Both scans resulted in the formation of the *Z* isomer of **5a** and **5b**. In the C-O bond formation scan, the barrier to this pathway is higher than simple isomerization of **4c** to **4a** (around 70 kJ mol^{-1}) followed by direct C-O bond formation (as described above) and so we conclude that this is not a competitive mechanism. However, in the C-N bond formation scan, the barrier to formation of **5b** appears to be lower than isomerization to **4b** (around 60 kJ mol^{-1}) and so this offers a lower energy pathway to **5b**, albeit one which is still much higher in energy than the formation of **5a** *via* the *O*-protonation pathway.

The stereoselectivity of the reaction, favoring the *E*-isomer of **5a**, appears to be a thermodynamic effect. Protonation of the β-carbon of the acetylide intermediate **3a** leads initially to a vinylidene **4a** that is primed for C-O bond formation *trans* to the C-R bond and formation of **5a_*Z***. However, this isomer lies 19 kJ mol^{-1} higher in energy than the *E*-isomer. Interconversion of the *E* and *Z* isomers of **5a** is possible *via* the vinylidene **4a** by rotation around the Ir=C bond,[47,48] and re-formation of the C-O bond. A low barrier to this rotation (around 10 kJ mol^{-1}) has been found (see ESI for details), so conversion of **5a_*Z*** to the more stable *E*-isomer would cost only around 73 kJ mol^{-1}, which is readily accessible under the reaction conditions. Proton transfer from the –N(H)R group of the protonated phosphoramidate to the acetylide leads directly from **3b** to **5b_*Z*** *via* $\mathbf{TS_{3b5b}}$. Although isomerization of **5b_*Z*** to **5b_*E*** is thermodynamically favorable, this would not be possible through a vinylidene

intermediate in a similar way to **5a**, as the relevant isomer (**4b**) lies 193 kJ mol^{-1} higher in energy than **5b_*Z***.

Table 1: Energies of isomer **5b**, relative to **5a**, with different alkyne substituents.

Alkyne R Group	**5b ΔG (kJ mol^{-1})**
Me	-6
Ph	1
p-^{t}Bu	3
Cy	-14
^{t}Bu	15

Substituent effects

As noted previously, it was observed that alkyne substituents do not appear to exert stereo- or regiocontrol.[22] Table 1 shows the relative energies of the regioisomers of **5a** and **5b** for different alkynes. For R = Me, Ph, and *p*-^{t}BuPh, the energy difference between the two products is negligible. For R = Cy and ^{t}Bu the energy difference is larger: 14 and 15 kJ mol^{-1} respectively. However, the thermodynamic product for these two substituents is reversed, with **5b** being the thermodynamic product when R = Cy and **5a** being favored when R = ^{t}Bu. In the case of R = ^{t}Bu, it is clear from the optimized structures (Figure 10) that there is a steric clash between the ^{t}Bu and *N*-2,6-dimethylphenyl groups in **5b(^{t}Bu)**, which causes some distortion of the structure that is evident in the larger < C-C(H)-C(^{t}Bu) angles (131 and 139^{o} for **5a** and **5b** respectively) and slightly longer Ir-N and C-C(H) distances. Presumably this disfavors products of type **5b**, resulting in **5a** being the most stable isomer. Based on the relatively small energy differences between the isomers in these data, it is likely that the experimental observation of **5a** rather than **5b** for all substituents is a kinetic, rather than thermodynamic effect, as discussed for R = Me above.

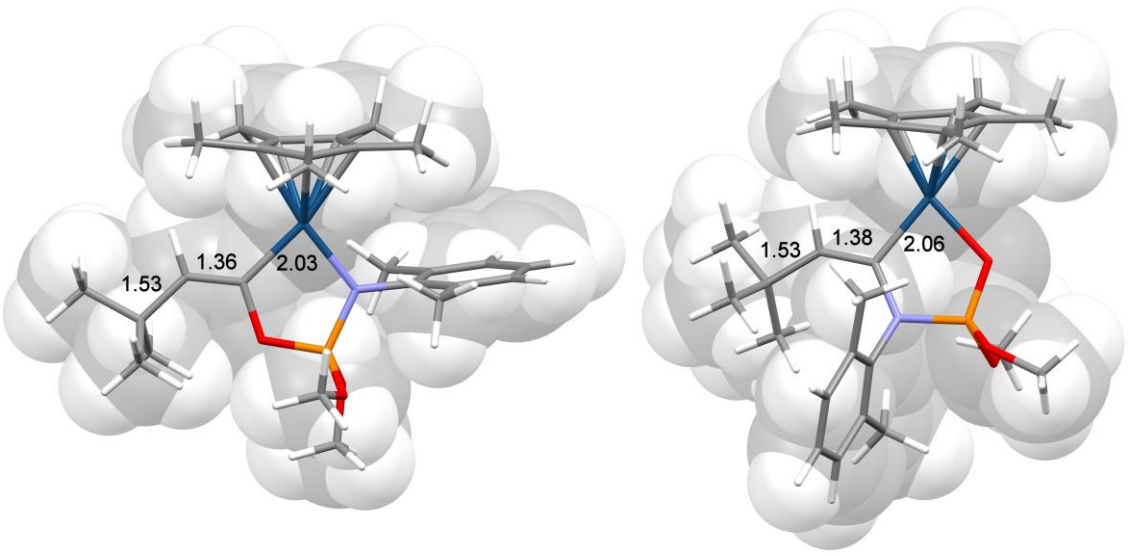

Figure 10: Optimized structures for **5a** (left) and **5b** (right) where R = ^{t}Bu on the alkyne, shown superimposed onto spacefill models of the complexes. Selected distances are shown in Å and the C-C(H)-C(^{t}Bu) angles are 131 and 139 ^{o} for **5a** and **5b** respectively. Dark blue = Ir, blue = N, orange = P, red = O, grey = C and white = H.

Conclusions

A detailed computational study has interrogated the mechanism, regio- and stereoselectivity for a recently reported phosphoramidate-assisted alkyne activation reaction at Ir(III). Five possible pathways for the formation of the observed five-membered vinyloxyirida(III)cycles were investigated to determine the most likely mechanism. Two of the five pathways: Cp*-protonation and oxidative addition to form an Ir(V) hydride, were found to have energy barriers that were much larger than the other pathways and are deemed unlikely to operate in this system. Of the remaining three pathways (direct 1,2-hydrogen migration and LAPS mechanisms involving *O*- or *N*-protonation) from the data discussed above, it is proposed that the reaction proceeds *via* a LAPS mechanism where the oxygen of the phosphoramidate phosphoryl (P=O) group serves as a proton shuttle, assisting in both C-H bond activation and C-H bond formation steps. Although we found the *N*-phosphoramidation product to be thermodynamically favored, this is not the product encountered experimentally and the present computational study suggests that this is due to a high-energy barrier for the LAPS mechanism *via N*-protonation, leading to the *N*-phosphoramidation isomer. The observed selectivity of the reaction for

the (*E*)-vinyloxyirida(III)cycle can be explained by its thermodynamic stability, compared to the (*Z*)-isomer, and the relatively low barrier to interconversion between them. Overall, this work highlights the mechanism by which a 1,3-heterobidentate chelating ligand shuttles protons, facilitating selective C-O bond formation with complete regio- and stereocontrol. Further, this work demonstrates the power of harnessing the hemilability of such ligands in an effort to provide a route for the development of new transformations *via* MLC.

Acknowledgements

The authors are grateful to the University of York (studentship for NML), the EPSRC (for computational equipment, EP/H011455/1 and EP/K031589/1), NSERC, and the government of Canada (Vanier scholarship for MWD) for funding. All data created during this research are available by request from the University of York Data Catalogue.

References

(1) Khusnutdinova, J. R.; Milstein, D. Metal–Ligand Cooperation. *Angew. Chem. Int. Ed.* **2015**, *54*, 12236.
(2) Eisenberg, R.; Gray, H. B. Noninnocence in Metal Complexes: A Dithiolene Dawn. *Inorg. Chem.* **2011**, *50*, 9741.
(3) Kaim, W.; Schwederski, B. Non-innocent ligands in bioinorganic chemistry-An overview. *Coord. Chem. Rev.* **2010**, *254*, 1580.
(4) Broere, D. L. J.; Plessius, R.; van der Vlugt, J. I. New avenues for ligand-mediated processes - expanding metal reactivity by the use of redox-active catechol, o-aminophenol and o-phenylenediamine ligands. *Chem. Soc. Rev.* **2015**, *44*, 6886.
(5) Tezgerevska, T.; Alley, K. G.; Boskovic, C. Valence tautomerism in metal complexes: Stimulated and reversible intramolecular electron transfer between metal centers and organic ligands. *Coord. Chem. Rev.* **2014**, *268*, 23.
(6) Gunanathan, C.; Milstein, D. Metal-Ligand Cooperation by Aromatization-Dearomatization: A New Paradigm in Bond Activation and "Green" Catalysis. *Acc. Chem. Res.* **2011**, *44*, 588.
(7) Luca, O. R.; Crabtree, R. H. Redox-active ligands in catalysis. *Chem. Soc. Rev.* **2013**, *42*, 1440.
(8) van der Vlugt, J. I.; Reek, J. N. H. Neutral Tridentate PNP Ligands and Their Hybrid Analogues: Versatile Non-Innocent Scaffolds for Homogeneous Catalysis. *Angew. Chem. Int. Ed.* **2009**, *48*, 8832.
(9) Noyori, R.; Hashiguchi, S. Asymmetric transfer hydrogenation catalyzed by chiral ruthenium complexes. *Acc. Chem. Res.* **1997**, *30*, 97.
(10) Davies, D. L.; Donald, S. M. A.; Al-Duaij, O.; Macgregor, S. A.; Polleth, M. Electrophilic C-H activation at {Cp*Ir}: Ancillary-ligand control of the mechanism of C-H activation. *J. Am. Chem. Soc.* **2006**, *128*, 4210.
(11) Qi, X.; Li, Y.; Bai, R.; Lan, Y. Mechanism of Rhodium-Catalyzed C–H Functionalization: Advances in Theoretical Investigation. *Acc. Chem. Res.* **2017**, *50*, 2799.

(12) Eisenstein, O.; Milani, J.; Perutz, R. N. Selectivity of C–H Activation and Competition between C–H and C–F Bond Activation at Fluorocarbons. *Chem. Rev.* **2017**, *117*, 8710.
(13) Lapointe, D.; Fagnou, K. Overview of the Mechanistic Work on the Concerted Metallation-Deprotonation Pathway. *Chem. Lett.* **2010**, *39*, 1119.
(14) Boutadla, Y.; Davies, D. L.; Macgregor, S. A.; Poblador-Bahamonde, A. I. Computational and synthetic studies on the cyclometallation reaction of dimethylbenzylamine with $[IrCl_2Cp^*]_2$: role of the chelating base. *Dalton Trans.* **2009**, , 5887.
(15) Crabtree, R. H. *The Organometallic Chemistry of the Transition Metals*; Fourth edition ed.; John Wiley & Sons, Inc.: Hoboken, New Jersey, 2005.
(16) Labinger, J. A.; Bercaw, J. E. Understanding and exploiting C-H bond activation. *Nature* **2002**, *417*, 507.
(17) Guihaume, J.; Halbert, S.; Eisenstein, O.; Perutz, R. N. Hydrofluoroarylation of Alkynes with Ni Catalysts. C-H Activation via Ligand-to-Ligand Hydrogen Transfer, an Alternative to Oxidative Addition. *Organometallics* **2012**, *31*, 1300.
(18) Davies, D. L.; Donald, S. M. A.; Macgregor, S. A. Computational study of the mechanism of cyclometalation by palladium acetate. *J. Am. Chem. Soc.* **2005**, *127*, 13754.
(19) Johnson, D. G.; Lynam, J. M.; Slattery, J. M.; Welby, C. E. Insights into the intramolecular acetate-mediated formation of ruthenium vinylidene complexes: a ligand-assisted proton shuttle (LAPS) mechanism. *Dalton Trans.* **2010**, *39*, 10432.
(20) Breit, B.; Gellrich, U.; Li, T.; Lynam, J. M.; Milner, L. M.; Pridmore, N. E.; Slattery, J. M.; Whitwood, A. C. Mechanistic insight into the ruthenium-catalysed anti-Markovnikov hydration of alkynes using a self-assembled complex: a crucial role for ligand-assisted proton shuttle processes. *Dalton Trans.* **2014**, *43*, 11277.
(21) de Aguirre, A.; Díez-González, S.; Maseras, F.; Martín, M.; Sola, E. The Acetate Proton Shuttle between Mutually Trans Ligands. *Organometallics* **2018**, 10.1021/acs.organomet.8b00417.
(22) Drover, M. W.; Love, J. A.; Schafer, L. L. Toward anti-Markovnikov 1-Alkyne O-Phosphoramidation: Exploiting Metal–Ligand Cooperativity in a 1,3-N,O-Chelated Cp*Ir(III) Complex. *J. Am. Chem. Soc.* **2016**, *138*, 8396.
(23) Arndt, M.; Salih, K. S. M.; Fromm, A.; Goossen, L. J.; Menges, F.; Niedner-Schatteburg, G. Mechanistic Investigation of the Ru-Catalyzed Hydroamidation of Terminal Alkynes. *J. Am. Chem. Soc.* **2011**, *133*, 7428.
(24) Huang, L.; Arndt, M.; Gooßen, K.; Heydt, H.; Gooßen, L. J. Late Transition Metal-Catalyzed Hydroamination and Hydroamidation. *Chem. Rev.* **2015**, *115*, 2596.
(25) Müller, F. *Agrochemicals: composition, production, toxicology, applications*; Wiley-VCH, 2000.
(26) Drover, M. W.; Bowes, E. G.; Schafer, L. L.; Love, J. A.; Weller, A. S. Phosphoramidate-Supported Cp*IrIII Aminoborane $H_2B{=}NR_2$ Complexes: Synthesis, Structure, and Solution Dynamics. *Chem. Eur. J.* **2016**, *22*, 6793.
(27) Drover, M. W.; Johnson, H. C.; Schafer, L. L.; Love, J. A.; Weller, A. S. Reactivity of an Unsaturated Iridium(III) Phosphoramidate Complex, $[Cp^*Ir\{\kappa^2\text{-}N,O\}][BAr_4^F]$. *Organometallics* **2015**, *34*, 3849.
(28) Drover, M. W.; Love, J. A.; Schafer, L. L. 1,3-N,O-Complexes of late transition metals. Ligands with flexible bonding modes and reaction profiles. *Chem. Soc. Rev.* **2017**, *46*, 2913.
(29) Drover, M. W.; Schafer, L. L.; Love, J. A. Capturing $HBCy_2$: Using N,O-Chelated Complexes of Rhodium(I) and Iridium(I) for Chemoselective Hydroboration. *Angew. Chem. Int. Ed.* **2016**, *55*, 3181.
(30) Drover, M. W.; Schafer, L. L.; Love, J. A. Dehydrogenation of cyclic amines by a coordinatively unsaturated Cp*Ir(III) phosphoramidate complex. *Dalton Trans.* **2017**, *46*, 8621.
(31) Csaszar, P.; Pulay, P. Geometry Optimization by Direct Inversion in the Iterative Subspace. *J. Mol. Struct.* **1984**, *114*, 31.
(32) Eichkorn, K.; Treutler, O.; Ohm, H.; Haser, M.; Ahlrichs, R. Auxiliary Basis-Sets to Approximate Coulomb Potentials. *Chem. Phys. Lett.* **1995**, *240*, 283.
(33) Eichkorn, K.; Weigend, F.; Treutler, O.; Ahlrichs, R. Auxiliary basis sets for main row atoms and transition metals and their use to approximate Coulomb potentials. *Theor. Chem. Acc.* **1997**, *97*, 119.

(34) von Arnim, M.; Ahlrichs, R. Geometry optimization in generalized natural internal coordinates. *J. Chem. Phys.* **1999**, *111*, 9183.
(35) Baldes, A.; Weigend, F. Efficient two-component self-consistent field procedures and gradients: implementation in TURBOMOLE and application to Au_{20}^-. *Mol. Phys.* **2013**, *111*, 2617.
(36) Klamt, A.; Schüürmann, G. COSMO Model. *J. Chem. Soc. Perkin Trans. 2* **1993**, 799.
(37) Schafer, A.; Klamt, A.; Sattel, D.; Lohrenz, J. C. W.; Eckert, F. COSMO Implementation in TURBOMOLE: Extension of an efficient quantum chemical code towards liquid systems. *Phys. Chem. Chem. Phys.* **2000**, *2*, 2187.
(38) Grimme, S.; Antony, J.; Ehrlich, S.; Krieg, H. A consistent and accurate ab initio parametrization of density functional dispersion correction (DFT-D) for the 94 elements H-Pu. *J. Chem. Phys.* **2010**, *132*, 154104.
(39) Grimme, S.; Ehrlich, S.; Goerigk, L. Effect of the Damping Function in Dispersion Corrected Density Functional Theory. *J. Comput. Chem.* **2011**, *32*, 1456.
(40) Deglmann, P.; Furche, F.; Ahlrichs, R. An efficient implementation of second analytical derivatives for density functional methods. *Chem. Phys. Lett.* **2002**, *362*, 511.
(41) Deglmann, P.; May, K.; Furche, F.; Ahlrichs, R. Nuclear second analytical derivative calculations using auxiliary basis set expansions. *Chem. Phys. Lett.* **2004**, *384*, 103.
(42) Maluendes, S. A.; Dupuis, M. A Dynamic Reaction Coordinate Approach to Abinitio Reaction Pathways - Application to the 1,5 Hexadiene Cope Rearrangement. *J. Chem. Phys.* **1990**, *93*, 5902.
(43) Ahlrichs, R.; Bar, M.; Haser, M.; Horn, H.; Kolmel, C. Electronic-Structure Calculations on Workstation Computers - the Program System Turbomole. *Chem. Phys. Lett.* **1989**, *162*, 165.
(44) Furche, F.; Ahlrichs, R.; Hattig, C.; Klopper, W.; Sierka, M.; Weigend, F. Turbomole. *WIREs Comput. Mol. Sci.* **2014**, *4*, 91.
(45) Cowley, M. J.; Lynam, J. M.; Slattery, J. M. A mechanistic study into the interconversion of rhodium alkyne, alkynyl hydride and vinylidene complexes. *Dalton Trans.* **2008**, , 4552.
(46) Biswas, B.; Sugimoto, M.; Sakaki, S. C-H bond activation of benzene and methane by M(eta(2)-O2CH)(2) (M = Pd or Pt). A theoretical study. *Organometallics* **2000**, *19*, 3895.
(47) Yang, S. Y.; Wen, T. B.; Jia, G. C.; Lin, Z. Y. Theoretical studies of rotational barriers of vinylidene ligands in the five-coordinate complexes $M(X)Cl(=C=CHR)L_2$ (M = Os, Ru; L = phosphine). *Organometallics* **2000**, *19*, 5477.
(48) Alireza, A.; Zare, K. Does type of phosphine affect rotational barrier of vinylidene in the complexes $OsHCl(C=CH_2)(L)_2$ (L = phosphine)? *Inorg. Chem. Commun.* **2004**, *7*, 999.

Supporting information statement

Full computational details, including tableted energies. Details of PES scans. Energiesand selected vibrational frequencies for all states. A text file of all computed Cartesian coordinates in xyz format for convenient visualization.

Conflict of interest statement

The authors declare no competing financial interests.